

CHAPTER 18

NEARSHORE CIRCULATION WITH 3-D PROFILES

Ib A. Svendsen,¹ Member, ASCE and Uday Putrevu,² Student Member, ASCE.

ABSTRACT

A model that predicts the depth variations of wave generated currents within the framework of a 2-D depth-integrated surf-zone model is described. The equations are formulated and solved for the case of a long, straight coast. The model is used to demonstrate that the effects of current refraction are weak and to determine the variation of the 3-D spiral shaped current profiles across the surf-zone. Finally, we show that the mixing coefficient required to get realistic variations of the longshore current is much larger than what the turbulence measurements can justify.

1. INTRODUCTION

The present paper describes a hydrodynamical model for 3-D wave generated currents in the nearshore region. The model is based on the idea of using a 2D-horizontal, depth integrated description to determine the integration constants in the analytical solutions for the vertical variation of the horizontal velocities. This idea was developed for the 2D cross-shore circulation by Svendsen & Hansen (1988). Independently, Davis (1987) pursued a similar idea for wind generated currents.

Quasi 3-D local solutions for current profiles were derived by deVriend & Stive (1987) based on dividing the flow into a primary and a secondary component. The more general approach used here was developed by Svendsen & Lorenz (1989) (S & L) who used a perturbation expansion to establish the equations. Concentrating on the longshore current profiles, they found that the equation normally used for the depth averaged longshore currents actually applies to the first approximation to the bottom velocity. The longshore velocity above bottom level increases uniformly, yielding somewhat (10-20%) larger depth averaged velocities at all locations than found by the classical depth integrated models.

In the present paper, the method of S & L is combined with the energy and cross-shore momentum equations to form a comprehensive computer model, the solution of which predicts wave heights, set-up, and, longshore and cross-shore currents and their variation over depth. For simplicity, the model equations are only established for a long cylindrical coast. This implies Snell's law is valid and it is possible to incorporate the wave-current refraction in the energy and

¹Professor, Center for Applied Coastal Research, Department of Civil Engineering, University of Delaware, Newark, DE 19716, USA

²Graduate Student, Center for Applied Coastal Research, Department of Civil Engineering, University of Delaware, Newark, DE 19716, USA

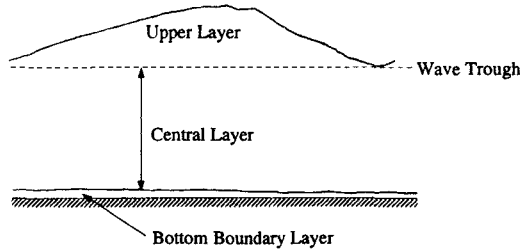


Figure 1: The three layer model concept

momentum equations in a simple manner. The basic equations of the model are described in Sections 2 and 3. This includes a description of how the bottom friction is incorporated as a boundary condition in the model.

On a long straight coast, the model equations become ordinary differential equations in x , the cross-shore coordinate. The energy and momentum equations represent initial value problems solved by specifying wave conditions at the seaward boundary. The longshore momentum equation is solved as a boundary value problem.

The system contains a number of features not previously included in such models though for reasons of limited space only a few of them can be analyzed and discussed here. In Section 4, we show that the wave-current interaction is really not modifying the wave motion or the current motion significantly even though the longshore current may be a substantial fraction of the wave speed. This is partly because the refractions due to the longshore and the cross-shore currents counteract each other, partly because the angle of incidence of the waves is usually small.

We also show the full cross-shore array of the 3-D spiral shaped current profiles corresponding to a given wave situation.

Finally, we confirm the logical conflict that still remains between which eddy viscosities are reasonable for the cross-shore circulation ($\nu_t \sim 0.01 h \sqrt{gh}$) and the many times larger coefficient for horizontal mixing required to achieve realistic variations of the longshore currents, particularly outside the surf zone for which we can find no justification in our knowledge about the turbulence characteristics. Though it has been suggested (Thornton & Guza, 1986) that on natural beaches this paradox may be accounted for by including the irregularity of wave breaking, that explanation does not cover experiments with regular waves where the effect seems equally strong (e.g., Visser 1982, 1984). Further examination of this problem would be desirable.

2. BASIC EQUATIONS FOR THE CURRENT VARIATION OVER DEPTH

The three layer model concept

The general approach is to utilize the concept of a 3 layer flow situation first suggested by Hansen & Svendsen (1984) and later used by Stive and Wind (1986) and Svendsen *et al.* (1987) (Fig. 1).

This approach assumes that there is a (mainly oscillatory) boundary layer at the bottom, within which the turbulence characteristics are dominated by the locally generated turbulence. In 2D cross-shore circulation, this assumption is

supported by the variation of current measurements and leads to very accurate results and there is no reason to expect the situation to be different in the general 3D case.

The method concentrates on the central or core layer, between the boundary layer and the wave trough. The third layer, between wave trough and wave crest, is considered separately from the middle layer because in that region there is water only part of the time, so we cannot separate the total particle velocity into an oscillatory and a mean (current) component.

In the central layer it is assumed that the turbulence is primarily produced by the breaking process. This means that it is both more intensive and has a larger length scale than the turbulence in the bottom boundary layer (Svendsen *et al.* 1987). This, in turn, justifies the assumption of a higher eddy viscosity ν_t in the central layer, based on the Prandtl-Kolmogorov assumption that

$$\nu_t \sim \ell \sqrt{q} \quad (1)$$

where q is the turbulent kinetic energy.

The basic equations

The general equations for the wave averaged (current) motion below trough level were derived by S & L. For a steady situation on a long straight coast, where $\partial/\partial y = 0$ (y being the shore parallel coordinate and x the shore normal coordinate pointing shorewards, see Fig. 2) those equations reduce to the following in the x and y directions, respectively:

$$\frac{\partial}{\partial z} \left(\nu_{tz} \frac{\partial U}{\partial z} \right) = \frac{\partial}{\partial x} \left(\overline{u_w^2} - \overline{w_w^2} + gb \right) + \frac{\partial \overline{u_w w_w}}{\partial z} + \frac{\partial U^2}{\partial x} \quad (2)$$

and

$$\frac{\partial}{\partial z} \left(\nu_{tz} \frac{\partial V}{\partial z} \right) = \frac{\partial \overline{u_w v_w}}{\partial x} + \frac{\partial \overline{v_w w_w}}{\partial z} + \frac{\partial UV}{\partial x} - \frac{\partial}{\partial x} \left(\nu_{tx} \frac{\partial V}{\partial x} \right) \quad (3)$$

Here $U(x, z)$, $V(x, z)$ are the cross and longshore current velocity components and u_w , v_w , w_w the oscillatory "wave" velocity components whose mean is zero below trough level. In (2) and (3) we have also modelled the turbulent shear stresses by introducing the eddy viscosity ν_t mentioned earlier. For later discussion we have distinguished between ν_{tx} and ν_{tz} . Reference is made to Fig. 2 for definitions of other variables.

It is inherent in the wave averaged approach that the wave particle velocities u_w , v_w and w_w are assumed known to the extent that the terms on the right hand side containing those parameters can be considered known.

Then (2) and (3) are actually two nonlinear equations for U and V . In classical models for nearshore circulation those terms are usually neglected because they are assumed small. To simplify the presentation, we will also neglect the nonlinear current terms. Furthermore, the findings from the perturbation solution by S & L justify that to the first approximation the horizontal mixing for the longshore current (last term in (3)) can be determined using the value V_b of V at the bottom.

Hence, as far as the depth variation of U, V is concerned, all terms on the right hand side of (2) and (3) are regarded as known forcing terms provided we can determine V_b . We define

$$\alpha_{1x}(x, z) = \frac{\partial}{\partial x} \left(\overline{u_w^2} - \overline{w_w^2} + gb \right) + \frac{\partial \overline{u_w w_w}}{\partial z} \quad (4)$$

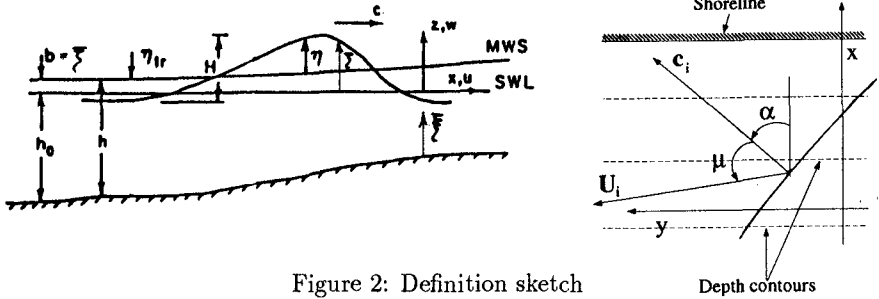


Figure 2: Definition sketch

$$\alpha_{1y}(x, z) = \frac{\partial \overline{u_w v_w}}{\partial x} + \frac{\partial \overline{u_w w_w}}{\partial z} - \frac{\partial}{\partial x} \left(\nu_{tx} \frac{\partial V_b}{\partial x} \right) \quad (5)$$

This means that (2) and (3) can be integrated directly, and the solutions written

$$U(x, z) = \int \frac{1}{\nu_{tz}} \int \alpha_{1x} d\xi d\xi + \int \frac{A_1}{\nu_{tz}} d\xi + A_2 \quad (6)$$

and the equivalent for V with α_{1y} instead of α_{1x} .

Thus (2) and (3) can be expressed in closed form for arbitrary α_1 and ν_{tz} . To simplify discussions, however, we will in the following assume $\nu_{tz}(x, z) = \nu_{tz}(x)$ and $\alpha_1(x, z) = \alpha_1(x)$. Hence, (6) simplifies to

$$U(x, z) = \frac{1}{2} \frac{\alpha_{1x}}{\nu_{tz}} \xi^2 + \frac{A_1}{\nu_{tz}} \xi + A_2 \quad (7)$$

$$V(x, z) = \frac{1}{2} \frac{\alpha_{1y}}{\nu_{tz}} \xi^2 + \frac{B_1}{\nu_{tz}} \xi + B_2 \quad (8)$$

where A_1, A_2, B_1 and B_2 are arbitrary functions of x to be determined from the boundary conditions discussed in the following and $\xi = z + h_o$ is the height above the bottom. To determine the four constants A_1, A_2, B_1 and B_2 we need two conditions for each of the two velocity components U and V .

The bottom boundary condition

The first condition used is related to the variation of U, V at the bottom. Strictly speaking, the bottom condition is $U, V = 0$. Due, however, to the assumption of a boundary layer with relatively low eddy viscosity a large value U_b, V_b of U, V exists at a short distance above the bottom (the “top” of the boundary layer). Hence, the mean bottom shear stress in the middle layer is related to U_b, V_b and to the oscillatory motion u_{wb}, v_{wb} at the bottom. We assume here that this relation is given by ($i = 1, 2$ corresponding to the x, y components)

$$\tau_{bi}(t) = \frac{1}{2} \rho f u_{bi}(t) | u_{bi}(t) | \quad (9)$$

where $u_{bi}(t)$ is the ensemble averaged bottom velocity, $| u_{bi} |$ the numerical value of u_{bi} and f is a (constant) friction factor (see, e.g., Jonsson 1966). For u_{bi} we have

$$u_{bi} = U_{bi} + u_{wbi} \quad (10)$$

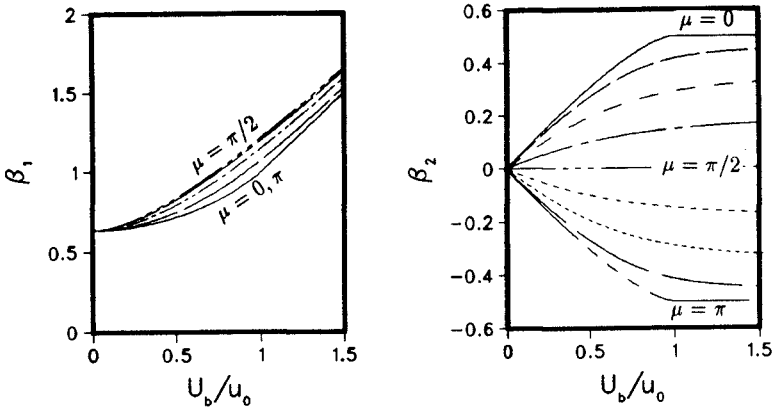


Figure 3: Variation of β_1 and β_2

where $U_{bi} = (U_b, V_b)$ and $u_{wbi} = (u_{wb}, v_{wb})$.

To determine the time mean of $\tau_{bi}(t)$, we also assume that

$$u_{wbi} = u_{oi} \cos \theta \quad (\theta = \omega t - kx) \tag{11}$$

and define, for short

$$u_o = |u_{oi}|, \quad U_b = |U_{bi}| \tag{12}$$

The mean shear stress $\tau_{bi} = \overline{\tau_{bi}(t)}$ is then determined by substituting (10), (11) and (12) into (9) and time averaging.

Liu and Dalrymple (1978) derived expressions for τ_{bi} for the special cases $U_b/u_o \gg 1$ (strong current) and $U_b/u_o \ll 1$ (weak current).

Here we present a more general formulation for arbitrary values of U_b/u_o and also arbitrary angles, μ , between the current direction and the wave direction. Performing the averaging operation we introduce the parameters

$$\beta_1 = \overline{\beta_1(t)} = \left[\left(\frac{U_b}{u_o} \right)^2 + 2 \frac{U_b}{u_o} \cos \theta \cos \mu + \cos^2 \theta \right]^{1/2} \tag{13}$$

$$\beta_2 = \overline{\beta_1(t) \cos \theta} \tag{14}$$

It then turns out that τ_{bi} can be written, without any further approximations, in the simple form

$$\tau_{bi} = \frac{1}{2} \rho f u_o [\beta_1 U_{bi} + \beta_2 u_{oi}] \tag{15}$$

which expresses τ_{bi} as the sum of two contributions, one in the direction of the current vector U_{bi} with weight β_1 , the other in the direction of the wave particle motion with weight β_2 . It is apparent from (13) and (14) that β_1 and β_2 are functions of two variables: U_b/u_o , the current strength relative to wave particle velocity amplitude and μ the angle between wave and current vectors. The variation of β_1 and β_2 with those parameters is shown in Fig. 3.

The expression (15) of course includes the cases of very weak and very strong currents. Though it is not apparent from (15), the case of $U_{bi} \rightarrow 0$ does yield $\tau_{bi} \rightarrow 0$: in purely sinusoidal motion there is no mean shear stress.

In the central layer the shear stress is given by

$$\tau_{zi} = \rho \nu_{tz} \frac{\partial U_i}{\partial z} \quad (16)$$

and for $z \rightarrow -h_o$ this shear stress must equal τ_{bi} determined from (15). Hence, combining (15) and (16) we get the mixed bottom boundary condition:

$$\frac{\partial U_i}{\partial z} - f(u_o, U_i) = 0 \quad z = -h_o \quad (17)$$

or, if we define

$$\begin{aligned} a &= \frac{1}{2} \frac{f}{\nu_{tz}} \beta_1 u_o \\ b_i &= \frac{1}{2} \frac{f}{\nu_{tz}} \beta_2 u_o u_{oi} \end{aligned} \quad (18)$$

and accept the slightly inconsistent nomenclature of $(\partial U_i / \partial z)_{-h_o} = \partial U_{bi} / \partial z$ then we can write (17) as the inhomogeneous mixed pseudo-linear condition for U_{bi}

$$\frac{\partial U_{bi}}{\partial z} - a U_{bi} = b_i \quad z = -h_o \quad (19)$$

This is the first of the boundary conditions used for the depth variation of U_i . Equation 19 is not quite linear because β_1 and β_2 depend on U_{bi} . It may also be noted that this implies that we can specify neither U_b nor τ_b at the bottom. It is the combination of U_b and τ_b imbedded in (19) that is controlled.

Applying (19) to the solutions (7) and (8) for U and V yields

$$U_i = \frac{1}{2} \frac{\alpha_{iz}}{\nu_{tz}} \xi^2 + (1 + a\xi) U_{bi} + b_i \xi \quad (20)$$

which expresses the vertical variation of the current velocity in terms of the unknown bottom velocity U_{bi} .

The second boundary condition

Hence, the function of the second boundary condition to be specified is essentially to determine the bottom velocity U_{bi} . The conditions used here are different in the longshore and in the cross-shore directions. In the longshore (y) direction, the second boundary condition is equivalent to specifying the shear stress τ_{sy} at wave trough level. τ_{sy} can be determined from the momentum balance for the flow above trough level (Stive and Wind 1986).

If the horizontal momentum flux above trough level is M_{ij} then we have

$$\tau_{sy} = \frac{\partial M_{xy}}{\partial x} \quad (21)$$

However, when combining the local depth variation of the flow given by (2) and (3) with a fully depth integrated model to give the horizontal variation it turns out to be more convenient not to impose (21) directly on the depth variation of the current. Instead, we apply the mixed condition (19) also to the fully depth integrated longshore momentum equation. This results, as shown in the next section, in an equation for the x variation of V_b , almost identical with the usual equation for the depth averaged longshore current. Solution of that equation therefore provides V_b and, hence, completely specifies the depth variation of the longshore component.

The question that naturally arises now is the following: Why is using the momentum equation integrated over the total depth to determine V_b completely equivalent to imposing (21) as a boundary condition for (20)? The explanation is the following: Determining the bottom velocity V_b from the total depth integrated momentum equation with (15) included means fixing the bottom shear stress so that depth integrated momentum is satisfied. At the same time, the solution (20) for V automatically accounts for the forcing that occurs below trough. Therefore, (20) with V_b determined as described will show a shear stress at trough level which corresponds exactly to (21) since τ_{sy} represents the difference between the total forcing and the forcing below trough level.

In the cross-shore direction, it is necessary to use a different approach. Because the cross-shore radiation stress is almost equal to the pressure gradient from the set-up, the method described above for V would lead to determining the bottom shear stress τ_{bx} as a (small) difference between these two large contributions (see Svendsen & Hansen, 1988). Instead we utilize that the net cross-shore flux Q_x is zero, so that

$$\int_{-h_o}^{\zeta_t} U dz = -Q_{sx}/(h_o + \zeta_t) \quad (22)$$

where Q_{sx} is the x -component of the mass flux in the wave, ζ_t is the trough elevation below SWL (Fig. 2).

Notice that this approach is only applicable for a straight coast where $\partial/\partial y$ and Q_x are zero. On a general coast we cannot distinguish between "cross-shore" and "longshore" and a different procedure is required.

3. THE DEPTH INTEGRATED EQUATIONS

The depth integrated equations are generalizations of the H-b model for calculation of the wave height H and set-up b in the surf zone first introduced by Svendsen (1984). That approach is based on dimensionless coefficients for radiation stress (P), energy flux (B), and energy dissipation (D). Using Phillips' (1977) equations the method was extended to 2D combination of waves and currents by Svendsen & Hansen (1986).

In most previous applications in the past the model has been applied using the special form of P , B and D found by incorporating experimental data for the real surface profile of the broken waves and including a roller contribution separately (Svendsen, 1984). The method as such, however, is general and by suitable choices of P , B and D can represent all H-b models. That was utilized by Hansen (1990) who specified empirical expressions for many of the surf-zone wave characteristics derived from actual measurements and found, not surprisingly, that they deviate substantially from sine-wave values. Here we use some of Hansen's results. The specific values of P , B and D used will be discussed further in connection with the applications (section 4).

We assume here that the waves are locally plane so that all wave properties can be described by 2-D wave theory. It is then convenient to define the momentum and pressure part of the radiation stress on a section perpendicular to the direction of wave propagation as the scalars

$$S_m = \overline{\int_{-h_o}^{\zeta} \rho u^2 dz} \quad (23)$$

$$S_p = -\overline{\int_{-h_o}^{\zeta} w_w^2 dz} + \frac{1}{2} \overline{\rho g (\zeta - \bar{\zeta})^2} \quad (24)$$

where $u^2 = u_w^2 + v_w^2$ is the horizontal wave particle velocity in the direction of wave propagation, ζ is the surface elevation above the horizontal axes.

We also define

$$e_{ij} = \begin{Bmatrix} \cos^2 \alpha & \sin \alpha \cos \alpha \\ \sin \alpha \cos \alpha & \sin^2 \alpha \end{Bmatrix} \quad (25)$$

where α is the direction of wave propagation relative to the x -axis (Fig. 2).

The radiation stress for a section with arbitrary normal vector then can be written

$$S_{ij} = e_{ij} S_m + \delta_{ij} S_p \quad (26)$$

where δ_{ij} is the Kroenecker δ . The generalized version of the dimensionless radiation stress P then is defined as

$$P_{ij} = \frac{S_{ij}}{\rho g H^2} = e_{ij} \frac{S_m}{\rho g H^2} + \delta_{ij} \frac{S_p}{\rho g H^2} \quad (27)$$

In particular, for our long straight coast we get

$$\begin{aligned} P_{xx} &= \frac{S_m}{\rho g H^2} \cos^2 \alpha + \frac{S_p}{\rho g H^2} \\ P_{xy} &= \frac{S_m}{\rho g H^2} \sin \alpha \cos \alpha \end{aligned} \quad (28)$$

Similarly, we define the dimensionless energy flux B by

$$E_{fi} = \rho g H^2 B c_i \quad (29)$$

where E_{fi} , the energy flux, is given by

$$E_{fi} = \overline{\int_{-h_o}^{\zeta} u_i \left[\rho g z + p + \frac{1}{2} \rho (u_w^2 + v_w^2 + w_w^2) \right] dz} \quad (30)$$

and

$$c_i = c \frac{k_i}{k} \quad (31)$$

k here represents the magnitude of the wavenumber vector, k_i .

Finally, we define the nondimensional energy dissipation D relative to the actual dissipation D by

$$D = D \cdot \frac{4hT}{\rho g H^3} \quad (32)$$

The three depth integrated equations solved are the cross-shore and the long-shore momentum equations, and the energy equation. We introduce the definitions above into the general equations of Phillips (1977) for waves and currents, simplifying to the conditions of a long straight coast including Snell's law. Finally, the dominating terms for H and b are isolated along the same lines as done by Svendsen & Hansen (1986) for the 2D cross-shore case. We then get, neglecting a few small terms, the depth integrated equations in the following form.

Cross-shore momentum equation

$$\frac{db}{dx} = - \left\{ \frac{P_{xx}}{h} [D' + g_1 + H^2 g_2] + \frac{\tau_{bx}}{\rho gh} \right\} \left(1 - \frac{1}{2} P_{xx} \cdot \left(\frac{H}{h} \right)^2 \right)^{-1} \quad (33)$$

where

$$g_1 = \left(\tau_{bi} U_{bi} - S_{xi} \frac{dU_i}{dx} - \frac{dUE}{dx} \right) / (\rho g c B \cos \alpha) \quad (34)$$

$$g_2 = \frac{1}{P_{xx}} \frac{dP_{xx}}{dx} - \frac{1}{2h} \frac{dh_o}{dx} - \frac{1}{B} \frac{dB}{dx} + \tan \alpha \frac{d\alpha}{dx} \quad (35)$$

$$D' = D / (\rho g c B \cos \alpha) \quad (36)$$

Energy equation

$$\frac{dH^2}{dx} = D' + g_1 - H^2 \left[\frac{1}{c} \frac{dc}{dx} + \frac{1}{B} \frac{dB}{dx} - \tan \alpha \frac{d\alpha}{dx} \right] \quad (37)$$

Longshore momentum equation

$$\frac{d}{dx} \int_{-h_o}^{\bar{n}} \nu_{tx} \frac{\partial V}{\partial x} dz - \frac{\tau_{by}}{\rho} = \frac{1}{\rho} \frac{dS_{xy}}{dx} \quad (38)$$

Solution of the equations

The desired equation for the bottom velocity V_b is found by substituting (15) and (20) into (38). Utilizing the findings of the perturbation solution developed by S & L, a first approximation to the resulting equation may be written

$$\frac{d}{dx} \left(\nu_{tx} h \frac{dV_b}{dx} \right) - a V_b = \frac{1}{\rho} \frac{dS_{xy}}{dx} + b_y \quad (39)$$

which is the differential equation we solve for V_b . The approximation made in (39) is that the turbulent mixing can be represented over the entire depth by using the bottom velocity V_b . The boundary conditions used for (39) are

$$V_b = 0 \quad \text{at} \quad x = x_{\text{shore}}, \rightarrow -\infty \quad (40)$$

Further, two matching conditions are used at the transition point x_t which is the point where the radiation stress starts to change. The matching conditions at x_t specify continuity in velocity and shear stress at x_t , that is:

$$V_{b+} = V_{b-}; \quad \nu_{tx+} \left(\frac{dV_b}{dx} \right)_+ = \nu_{tx-} \left(\frac{dV_b}{dx} \right)_- \quad \text{at} \quad x_t$$

where + and – refer to values immediately adjacent to x_i . Outside the surf-zone, dS_{xy}/dx is zero.

4. RESULTS

The 3D model system established above can be used to study a number of effects on a long straight coast which has not been analyzed previously in the literature. For reasons of limited space, the discussion is limited to a few mechanisms.

The numerical results will depend on the wave incidence angle α , the bottom slope h_{ox} (here assumed constant for simplicity, not necessity), and the way the wave properties are modelled, as a function of wave height, including the breaking criteria. Following Svendsen (1987), we have chosen to assume that the breaker height is given by $(H/h)_b = 1.11 \cdot (h_x L/h)_b^{1/4}$. An almost identical expression was suggested independently by Hansen (1990). The vertical eddy viscosity, ν_{tz} , was taken to be $\nu_{tz} = 0.01 h \sqrt{gh}$ (a discussion of the eddy viscosity is given later). The horizontal eddy viscosity, ν_{tx} , was taken to be $\nu_{tx} = 0.01 h \sqrt{gh}/h_x$.

The wave parameters—energy flux (B) and radiation stress (P)—depend on the shape of the surface profile and the area of the roller (Svendsen 1984). The shape of the surface profile is measured in terms of the dimensionless parameter B_o defined as $B_o = (\eta/H)^2$. In the present applications these parameters have been derived using the B_o suggested by Hansen (1990) and modified for waves with a current as in Svendsen & Hansen (1986), and the roller area found by Okayasu (1989). The dimensionless energy dissipation rate is taken to be the same as in a bore. The reason for choosing this set of parameters is that in this way we include the actual characteristics of broken waves. Usually, this model gives the best prediction of the set-up, which means of dS_{xx}/dx . Since S_{xy} through (25) and (26) is related to S_{xx} , it is evident that this also potentially implies a better prediction of the driving force for the longshore current. This point is important though it is usually disregarded in the discussions of surf zone wave theories and longshore currents.

Wave-current refraction

Many of the measurements of longshore currents both in the field and in the laboratory show very high velocities. The steeper the local bottom slope, the higher the velocity. For a coast with a slope of 1:30, velocities typically correspond to a Froude number of 0.2–0.4 or longshore velocities of 20–40% of the wave celerity. Visser in his experiments on 1:20 and 1:10 slope beaches obtained velocities corresponding to Froude numbers as large as 0.7–1.2; i.e., current velocities equal to or higher than the propagation speed of the waves. Wave current refraction is caused by the gradient in current velocity so one would expect a strong change in the wave pattern and hence on the current itself from this mechanism.

Dalrymple (1980) used a perturbation expansion to examine the simplified case of no turbulent mixing. The present model includes both turbulent mixing and the additional effect of the undertow. Based on Kirby & Chen (1989), this cross-shore current is represented by the mean value of the velocity below trough level.

Fig. 4a shows the changes in wave incident angle for a case with slope 1:30, deep water incident angle $\alpha_o = 15^\circ$. Four cases are shown: No current refraction, longshore current only, undertow only, and the full 3D case with both longshore and cross-shore flow. It is seen that the effects of the cross and the longshore

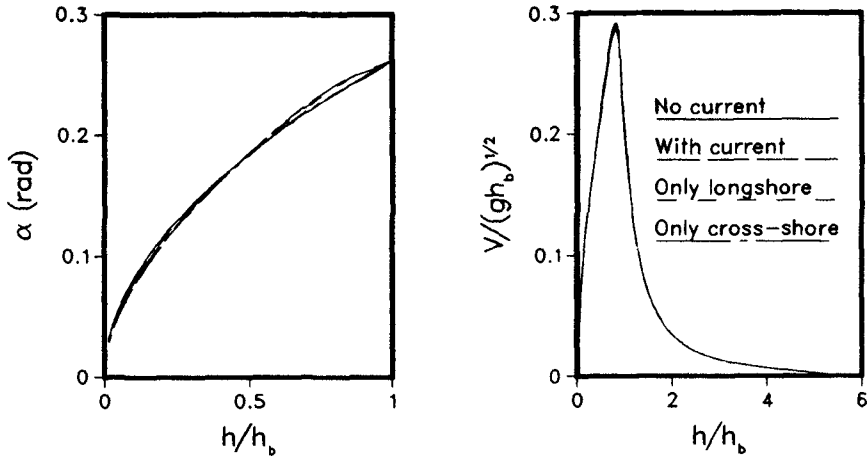


Figure 4: Effect of current refraction

currents counteract and almost cancel each other. Also, the effect of each of the two factors isolated is actually very modest. This is also clear from the resulting longshore current profiles shown in Fig. 4b. The effect of the current refraction is only just discernible at the peak of the velocity distribution even if the undertow is neglected.

Steeper slopes and larger angles of incidence will increase the effect and so will a 3D circulation pattern that locally creates a significant shoreward flow. Even then, however, our computations suggest that wave current refraction is not a very important mechanism for changing the current velocities.

Velocity profiles

Another feature of the present model is its capability of supplying the fully 3-dimensional velocity profiles from the 2-D horizontal, depth integrated solutions to equations (32)–(35).

The generic form of the velocity profiles was shown by S & L. As is apparent from the model, however, to obtain the profiles pertaining to each location it is necessary first to calculate the wave height and setup variation described by (32) and (33). In many previous nearshore models this part is eliminated by simply assuming that the wave height is a constant fraction γ of the waver depth.

Fig. 5 shows a set of consecutive 3D current profiles in the surf zone for a situation with slope $h_{ox} = 1/30$, and angle of incidence at the breakpoint of $\alpha_b = 5^\circ$. To obtain equal detailing, each profile has been scaled relative to the local depth under wave trough and the local wave celerity. We see that in the region where the longshore current is largest the bottom velocity is predominantly longshore, but in other regions the cross-shore motion is more prevailing.

If the angle of incidence increases, the longshore current velocity increases similarly and hence prevails more. Similarly, on a steeper slope, the cross-shore motion becomes stronger.

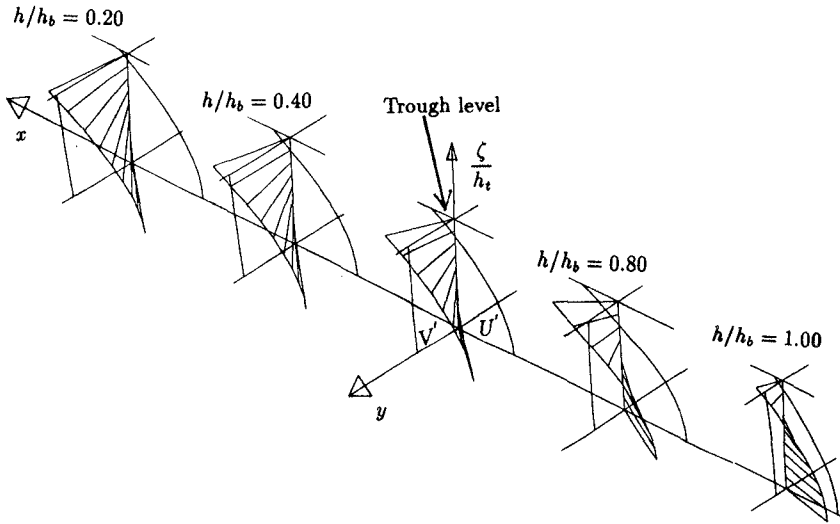


Figure 5: Variation of the velocity profiles across the surf-zone

Eddy viscosity

The eddy viscosity, ν_{tz} , in the surf-zone has been determined previously by fitting computed undertow profiles to measured data. Values reported range from $0.007h\sqrt{gh}$ through $0.03h\sqrt{gh}$ (Svendsen and Hansen 1988) to a linear variation between zero and $0.3h_x h\sqrt{gh}$ (Okayasu *et al.* 1988), the later yielding $0.01h\sqrt{gh}$ for $h_x = 1/30$.

In contrast, the eddy viscosity, ν_{tx} used by, e.g., Longuet-Higgins (1970) for longshore currents is equivalent to $0.01h\sqrt{gh}/h_x$, which on $1/30$ yields $0.3h\sqrt{gh}$ or about 30 times the value that can be justified for the undertow even inside the surf-zone. The large absolute value of $\nu_{tx} = 0.3h_b\sqrt{gh_b}$ at the breaker point is required to apply everywhere outside that point, and our comparison with Visser's (1982) measurements for regular waves confirm that such a large eddy viscosity is necessary to make the computations match with the measurements. Figure 6 shows that the difference obtained in the longshore current distribution using ν_{tx} equal to the ν_{tz} value found from undertow and ν_{tx} given by the Longuet-Higgins value mentioned above is very substantial.

On the other hand, if we combine the hypothesis described by (1) for the nature of the mechanism behind ν_t with the fact that outside the surf-zone the turbulence is rather weak, it becomes inconceivable that this mixing mechanism can be due to turbulence. In this context, it is interesting that Thornton and Guza (1986) find that the effect of the eddy viscosity in their NSTS data from Santa Barbara is negligible in comparison to the variability of the waves even during periods of narrow banded, almost unidirectional incident waves. In other words, a physically realistic eddy viscosity would still give correct results. However, this does not explain which mechanism causes a similar mixing in the regular wave experiments. It is beyond the space available to discuss possible explanations to

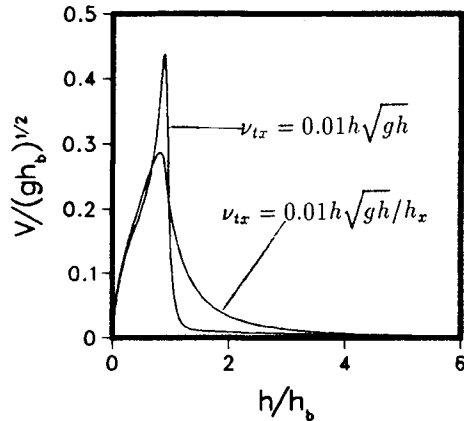


Figure 6: Effect of eddy viscosity

this paradox. What we seem to be able to conclude at this moment is that a very strong mixing process is controlling the longshore current distribution outside the breaker point both in regular and irregular waves.

ACKNOWLEDGEMENTS

This work is part of a project funded by the National Sea Grant Program. The authors wish to thank A. Wurjanto (University of Delaware) for his help with the graphics.

REFERENCES

- Davies, A. M., 1987. On extracting current profiles from vertically integrated numerical models. *Coastal Engineering*, 11, pp. 445-477.
- Dalrymple, R. A., 1980. Longshore currents with wave current interaction. *Journal of Waterway, Port, Coastal, and Ocean Engineering*. Vol. 106, No. WW3, pp. 414-420.
- deVriend, H. J. and M. J. F. Stive, 1987. Quasi-3D modelling of nearshore currents. *Coastal Engineering*, 11, pp. 565-601.
- Hansen, J. B., 1990. Periodic waves in the surf-zone: Analysis of experimental data. *Coastal Engineering*, 14, pp. 19-41.
- Hansen, J. B. and I. A. Svendsen, 1984. A theoretical and experimental study of the undertow. *Proc. 19th ICCE, Houston*. pp. 2246-2262.
- Jonsson, I. G., 1966. Wave boundary layers and friction factors. *Proc. 10th ICCE, Tokyo*. pp. 127-148.
- Kirby, J. T. and T.-M. Chen, 1989. Surface waves on vertically sheared flows: Approximate dispersion relations. *Journal of Geophysical Research*, 94 (C1), pp. 1013-1027.
- Liu, P. L.-F. and R. A. Dalrymple, 1978. Bottom frictional stresses and longshore currents due to waves with large angles of incidence. *Journal of Marine Research*, 36, pp. 357-375.
- Longuet-Higgins, M. S., 1970. Longshore currents generated by obliquely incident sea waves. Part 2. *Journal of Geophysical Research*, 75, pp. 6790-6801.

- Okayasu, A., 1989. Characteristics of turbulence structure and undertow in the surf-zone. Doctoral dissertation, University of Tokyo, 119 pp.
- Okayasu, A., T. Shibayama and K. Horikawa, 1988. Vertical variation of undertow in the surf-zone. Proc. 21st ICCE, Costa del Sol-Magala. pp. 478-491.
- Phillips, O. M., 1977. The dynamics of the upper ocean. Cambridge University Press, 336 pp.
- Stive, M. J. F. and H. G. Wind, 1986. Cross-shore mean flow in the surf-zone. Coastal Engineering, 6, pp. 325-340.
- Svendsen, I. A., 1984. Wave heights and set-up in a surf-zone. Coastal Engineering, 8, pp. 303-329.
- Svendsen, I. A., 1987. Analysis of surf-zone turbulence. Journal of Geophysical Research, 92 (C5), pp. 5115-5124.
- Svendsen, I. A. and J. B. Hansen, 1986. Interaction of waves and currents over a longshore bar. Proc. 20th ICCE, Taipei. pp. 1580-1594.
- Svendsen, I. A. and J. B. Hansen, 1988. Cross-shore currents in surf-zone modelling. Coastal Engineering, 12, pp. 23-42.
- Svendsen, I. A. and R. S. Lorenz, 1989. Velocities in combined undertow and longshore currents. Coastal Engineering, 13, pp. 55-79.
- Svendsen, I. A., H. A. Schaffer and J. B. Hansen, 1987. The interaction between the undertow and the boundary layer flow on a beach. Journal of Geophysical Research, 92 (C11), pp. 11845-11856.
- Thornton, E. B. and R. T. Guza, 1986. Surf-zone longshore currents and random waves: Field data and models. Journal of Physical Oceanography, 16, pp. 1165-1178.
- Visser, P. J., 1982. The proper longshore current in a wave basin. Communications on Hydraulics. Report 82-1, Dept. of Civil Engineering, Delft Univ. of Technology, 86 pp.
- Visser, P. J., 1984. A mathematical model of uniform longshore currents and comparison with laboratory data. Communications on Hydraulics. Report 84-2, Dept. of Civil Engineering, Delft Univ. of Technology, 151 pp.